

# Absorption resonance and large negative delay in Rb vapor with buffer gas.

Eugeniy E. Mikhailov,\* Vladimir A. Sautenkov, Yuri V. Rostovtsev, and George R. Welch

*Department of Physics and Institute of Quantum Studies,  
Texas A&M University, College Station, Texas 77843-4242*

(Dated: November 2, 2018)

We observe a narrow, isolated, two-photon absorption resonance in  $^{87}\text{Rb}$  for large one-photon detuning in the presence of a buffer gas. In the absence of buffer gas, a standard  $\Lambda$  configuration of two laser frequencies gives rise to electromagnetically induced transparency (EIT) for all values of one-photon detuning throughout the inhomogeneously (Doppler) broadened line. However, when a buffer gas is added and the one-photon detuning is comparable to or greater than the Doppler width, an absorption resonance appears instead of the usual EIT resonance. We also observe large negative group delay ( $\approx -300 \mu\text{s}$  for a Gaussian pulse propagating through the media with respect to a reference pulse not affected by the media), corresponding to a superluminal group velocity  $v_g = -c/(3.6 \times 10^6) = -84 \text{ m/s}$ .

PACS numbers: 270.1670, 270.5530

Quantum coherence effects have attracted great attention the last few years. Phenomena such as ultra-low optical group velocity [1, 2, 3, 4], super-luminal group velocity [4, 5, 6], enhanced nonlinear optical effects [7], and quantum information storage [8, 9, 10] have all been studied under the condition of electromagnetically induced transparency (EIT) [11]. More recently, complementary coherence effects such as electromagnetically induced absorption (EIA) have been predicted and studied [6, 12, 13, 14]. In the Letter, we present the experimental observation of a new narrow absorption resonance appearing at large optical density and large detuning in Doppler broadened media with buffer gas.

In typical experiments, the narrow transmission linewidth in EIT is limited by the relaxation rate of the ground-state coherence, which is usually determined by the interaction time of an atom with the applied laser radiation. Two common methods for increasing the interaction time are by use of wall coatings [15] that allow an atom to maintain its coherence while it travels into and out of the interaction region many times, and by use of a buffer gas that allows the atom to diffuse out of the interaction region slowly by velocity changing collisions that still preserve the ground-state coherence [16, 17].

For a  $\Lambda$ -type EIT system, the dependence of the EIT resonance on one-photon laser detuning has been studied experimentally [18] and theoretically [19]. They show that in the limit of high buffer gas pressure, when the decay rate of the upper level is comparable with the Doppler broadening, the EIT resonance shape can be described by a Lorentzian plus a dispersion-like curve:

$$f(\delta) = \gamma \frac{A\gamma + B(\delta - \delta_0)}{\gamma^2 + (\delta - \delta_0)^2} + C \quad (1)$$

where  $\gamma$  is the width of the resonance,  $\delta$  is the two photon detuning,  $\delta_0$  is one-photon dependent resonance shift with respect to resonance position for zero one-photon detuning,  $A$  is the amplitude of the Lorentzian part,  $B$

is the amplitude of the dispersion-like part, and  $C$  is an offset. However previous experimental studies [18] have only seen the resonance shape become somewhat assymmetric while still maintaining an EIT resonance-like shape, in other words  $A > 0$  and  $|B/A| < 2$ .

In our experiment we achieve an absorption-like resonance ( $A < 0$ ) by detuning the drive laser into the wings of the Doppler distribution in a cell with buffer gas. For our conditions, no absorption is found without buffer gas. The absorption resonance is accompanied by large anomalous dispersion so that negative group delay is observed for a pulse propagating through the medium. It is important to stress that the previous observation of EIA in Refs. [6, 12, 13, 14] and the enhanced absorption seen in the Hanle effect [20] have a different nature than what we observe here, since those previous observations require that the degeneracy of the ground state be lower than that of the excited state [13], (i.e.  $F < F'$ ) for a drive field transition, which is not necessary in our experiments.

We use a weak probe and a strong drive (or coupling) field in a  $\Lambda$  configuration of the two ground-state levels  $5S_{1/2}F = 1, 2$  and the excited  $5P_{1/2}F = 2$  state of  $^{87}\text{Rb}$  as shown in Fig. 1. We operate in the power-broadened regime where  $\Omega_d > \sqrt{\gamma\gamma_{bc}}$  where  $\Omega_d$  is the drive laser Rabi frequency,  $\gamma$  is the radiative decay rate as defined above, and  $\gamma_{bc}$  is the decay rate of ground-state coherence. The resulting ground-state coherence gives rise to a narrow EIT resonance of the probe field in the vicinity of two-photon resonance ( $\delta = 0$ ). This coherence still exists even for one-photon detunings ( $\Delta$ ) comparable to or somewhat greater than the inhomogeneous Doppler width of the medium.

Because of the way our probe field is generated (discussed below) a second  $\Lambda$  configuration consisting of a weak Stokes component and the drive field (see Fig. 1) also is present. However, this system is detuned far from resonance, and does not affect our system notably.

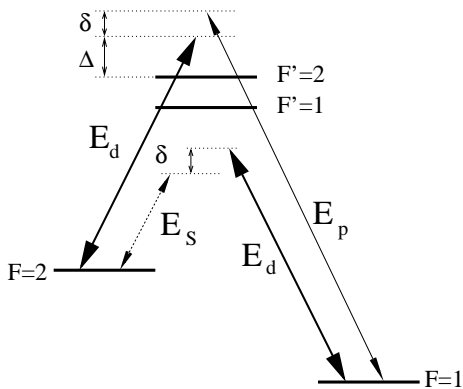


FIG. 1: Three-level interaction scheme of three laser fields with  $^{87}\text{Rb}$  atoms. The long-lived coherence is created on the hyperfine split ground-state sublevels with a strong driving field  $E_d$  and a weak probe field  $E_p$ . A weak Stokes field  $E_s$  is also present as a by-product of the generation of the probe field.  $\Delta$  is the one-photon detuning of the drive and probe laser from their respective atomic transitions, and  $\delta$  is the two-photon detuning, which is scanned.

(Nonetheless, the propagation properties of the Stokes component are rather interesting and will be discussed elsewhere.)

Our experimental setup is shown schematically in Fig. 2. We use an external cavity diode laser tuned to the vicinity of the  $5S_{1/2} \rightarrow 5P_{1/2}$  ( $D_1$ ) transition of  $^{87}\text{Rb}$ . The laser is referred to as the driving field ( $E_d$ ) in Fig. 1. Detuning of the drive laser ( $\Delta$ ) changes from zero up to 2 GHz and is always positive (for any  $\Delta > 0$  detuning from upper levels  $F' = 1, 2$  is larger than for zero detuning as it shown in Fig. 1). Sidebands are generated on the drive laser by an electro-optic modulator (EOM) which is tunable in the vicinity of the 6.835 GHz ground state splitting. The drive laser is tuned to the  $F = 2 \rightarrow F' = 2$  transition so that the upper sideband serves as the probe field, and is tunable in the vicinity of the  $F = 1 \rightarrow F' = 2$  transition. The lower sideband (Stokes component) is far off resonance. After the EOM, all fields pass through a single-mode optical fiber to obtain a clean Gaussian spatial mode. The laser is collimated to a diameter of 7 mm, and circularly polarized with a  $\lambda/4$  wave-plate right before the cell. The cell itself is surrounded by 3 layer magnetic shield which suppresses the laboratory magnetic field. The cell is heated to  $60 - 70^\circ\text{C}$  to control the density of  $^{87}\text{Rb}$  vapor.

Before the EOM, part of the drive laser is split from the main beam, shifted in frequency by a small amount (60 MHz) with an acousto-optic modulator and deflected around the cell. This shifted beam is recombined with the light transmitted through the cell and all the fields are detected on a fast photodiode. This (heterodyne) procedure allows us to separately detect the transmitted probe and Stokes fields. [2].

We measure the EIT spectrum (transmission as a func-

tion of two-photon detuning  $\delta$  for various one photon detunings of the driving field ( $\Delta$ ). We also measure the group delay of a pulse propagating through the cell. This is done with a programmable pulse synthesizer, which modulates the microwave generator for the EOM. We thus produce a Gaussian (temporal) pulse in the power of the drive field sidebands (the probe field). The delay time is extracted by data taking and analyzing software on a computer which collects the separate probe and reference signals.

We first measure various transmission spectra for a  $^{87}\text{Rb}$  cell with no buffer gas. Our measurements, shown in Fig. 3a show that the EIT resonance maintains its transmission-like shape as the drive and probe are detuned from one-photon resonance. When the lasers are far from resonance (bottom trace in Fig. 3a), the lasers interact with a very small number of atoms, and the width of the EIT resonance is determined by power broadening by the drive laser (width  $\approx \Omega^2/\gamma$  where  $\Omega$  is the drive Rabi frequency and  $\gamma$  is the Doppler width). When the lasers are on resonance, the effective optical density is much higher, and the EIT width is much lower than the power-broadened width [21, 22, 23].

Next we replace the vacuum cell by a cell with 30 Torr of Ne buffer gas. Results are shown in Fig. 3b. We find that the resonance spectra for large one-photon detuning ( $\Delta$ ) are changed dramatically from the vacuum case just described. We see that as the one-photon detuning is increased, the EIT resonance passes through a dispersion-like shape and into an absorption-like shape.

Second, we find that this absorption-like resonance is accompanied by steep anomalous dispersion which results in a large negative propagation delay of the probe pulse with respect to a reference pulse that is not delayed by the medium. Sample pulses are shown in Fig. 4. These data show a  $-300 \mu\text{s}$  delay produced by a 2.5 cm long cell, implying a superluminal group velocity  $v_g = -84 \text{ m/s}$ .

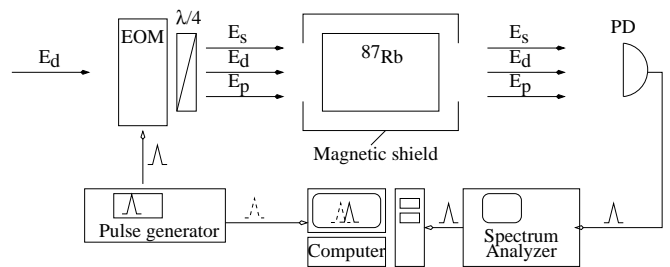


FIG. 2: Schematic of the experimental setup.

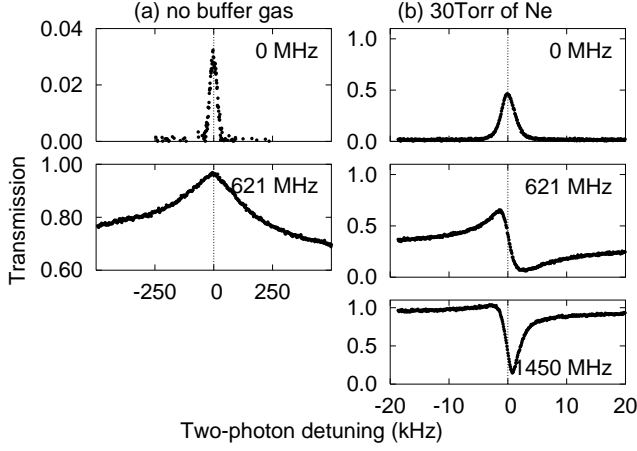


FIG. 3: Transmission of probe field as a function of two-photon detuning  $\delta$  (measured in kHz) for various one-photon detunings  $\Delta$ . (a)  $^{87}\text{Rb}$  cell with no buffer gas (vacuum). (b)  $^{87}\text{Rb}$  cell with 30 Torr of Ne. The vertical scales are normalized in such a way that 0 correspond to zero transmission and 1 correspond to zero absorption (or total transparency). Experimental parameters: (a)  $T = 66.4^\circ\text{C}$ ,  $N = 4.2 \times 10^{11} \text{ cm}^{-3}$ ; Total power into cell  $630 \mu\text{W}$ , out  $40 \mu\text{W}$ ; cell length = 4.7 cm. (b)  $T = 67.7^\circ\text{C}$ ,  $N = 4.7 \times 10^{11} \text{ cm}^{-3}$ ; Total power into cell  $\approx 400 \mu\text{W}$ ; cell length = 2.5 cm.

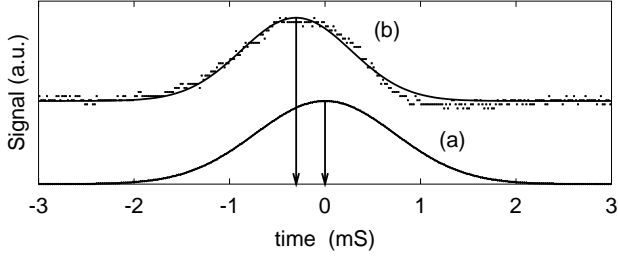


FIG. 4: Demonstration of negative pulse delayed time. (a) The probe field is given a Gaussian temporal pulse shape. (b) The transmitted probe field, showing negative time delay before transmission. Experimental conditions same as for Fig. 3b.

In order to gain physical insight into this new phenomenon we have made numerical simulations based on the density matrix equations coupled with a Maxwell equation description of propagation effects in steady state for low intensity of the probe field. For numerical simulation we use a 3-level atomic model coupled with probe and drive fields ( $\Lambda$  scheme).

The density matrix equations are the following:

$$\dot{\rho}_{bb} = i\Omega_p^* \rho_{ab} - i\Omega_p \rho_{ba} + \gamma_r \rho_{aa} - \gamma_{bc} \rho_{bb} + \gamma_{bc} \rho_{cc}, \quad (2)$$

$$\dot{\rho}_{cc} = i\Omega_d^* \rho_{ac} - i\Omega_d \rho_{ca} + \gamma_r \rho_{aa} - \gamma_{bc} \rho_{cc} + \gamma_{bc} \rho_{bb}, \quad (3)$$

$$\dot{\rho}_{ab} = -\Gamma_{ab} \rho_{ab} + i\Omega_p (\rho_{bb} - \rho_{aa}) + i\Omega_d \rho_{cb}, \quad (4)$$

$$\dot{\rho}_{ca} = -\Gamma_{ca} \rho_{ca} + i\Omega_d^* (\rho_{aa} - \rho_{cc}) - i\Omega_p^* \rho_{cb}, \quad (5)$$

$$\dot{\rho}_{cb} = -\Gamma_{cb} \rho_{cb} - i\Omega_p \rho_{ca} + i\Omega_d^* \rho_{ab}, \quad (6)$$

where  $\Omega_d = \wp_{ac} E_p / \hbar$  and  $\Omega_p = \wp_{ab} E_d / \hbar$  are the Rabi frequencies of the drive and probe fields. The generalized decay rates are defined as:

$$\Gamma_{ab} = \gamma + i(\Delta + \delta), \quad (7)$$

$$\Gamma_{ac} = \gamma + i\Delta, \quad (8)$$

$$\Gamma_{cb} = \gamma_{bc} + i\delta. \quad (9)$$

Here  $\gamma = \gamma_r + \gamma_p$  is the polarization decay rate,  $\gamma_r$  is the radiative decay rate of the excited state,  $\gamma_p$  is dephasing rate, and  $\gamma_{bc}$  is the inverse lifetime of the coherence between ground states  $|b\rangle$  and  $|c\rangle$ . Here we recall that the presence of the buffer gas affects values of both  $\gamma_{bc}$  and  $\gamma$ . On one hand, as mentioned above, it allows preservation of the ground-state coherence longer, but on the other hand it broadens the optical transition, since  $\gamma_p$  grows linearly with buffer gas pressure [24].

Solving these equations in the steady state regime and assuming  $|\Omega_p| \ll |\Omega_d|$ , we obtain the following expression for the linear susceptibility of the probe field:

$$\chi_{ab}(\Delta) = i\eta \frac{\Gamma_{cb}(\rho_{aa}^{(0)} - \rho_{bb}^{(0)}) + \frac{|\Omega_d|^2}{\Gamma_{ca}}(\rho_{aa}^{(0)} - \rho_{cc}^{(0)})}{\Gamma_{ab}\Gamma_{cb} + |\Omega_d|^2}, \quad (10)$$

where  $\eta = \frac{3}{8\pi} N \lambda^2 \gamma_r$ ,  $N$  is the  $^{87}\text{Rb}$  density,  $\lambda$  is the wavelength of the probe field, and  $\rho_{aa}^{(0)}$ ,  $\rho_{bb}^{(0)}$ ,  $\rho_{cc}^{(0)}$  are the solution of above equations in case when  $\Omega_p = 0$ . Then to take into account propagation and Doppler averaging, the Maxwell equation is given by

$$\frac{\partial \Omega_p}{\partial z} = -i\Omega_p \int \chi_{ab}(\Delta + kv) dv \quad (11)$$

has been solved numerically, where  $k$  is the wavenumber of either probe or drive field.

We model the effect of the buffer gas by adding an additional homogeneous broadening for the optical transitions  $\gamma_p$  and decreasing of the time-of-flight limit for the hyperfine coherence decay rate  $\gamma_{bc}$  based on the atomic diffusion in the buffer gas. In our simulation for EIT in the absence of buffer gas, we use  $\gamma_p = 0$  and  $\gamma_{bc}/2\pi = 10 \text{ kHz}$ . For our simulation of the effects of buffer gas, we use  $\gamma_p/2\pi = 120 \text{ MHz}$  and  $\gamma_{bc}/2\pi = 1 \text{ kHz}$ . The results of these simulations are shown in Fig. 5 agree well with the experimental results of Fig. 3. We model the effect of the buffer gas by adding an additional homogeneous broadening for the optical transitions  $\gamma_p$  using the cross-sections for broadening from [25] and decreasing of the time-of-flight limit for the hyperfine coherence decay rate  $\gamma_{bc}$  based on the atomic diffusion in the buffer gas [25]. In our simulation for EIT in the absence of buffer gas, we use  $\gamma_p = 0$  and  $\gamma_{bc}/2\pi = 10 \text{ kHz}$ . For our simulation of the effects of buffer gas, we use  $\gamma_p/2\pi = 120 \text{ MHz}$  and  $\gamma_{bc}/2\pi = 1 \text{ kHz}$  [25]. The results of these simulations are shown in Fig. 5 agree well with the experimental results of Fig. 3.

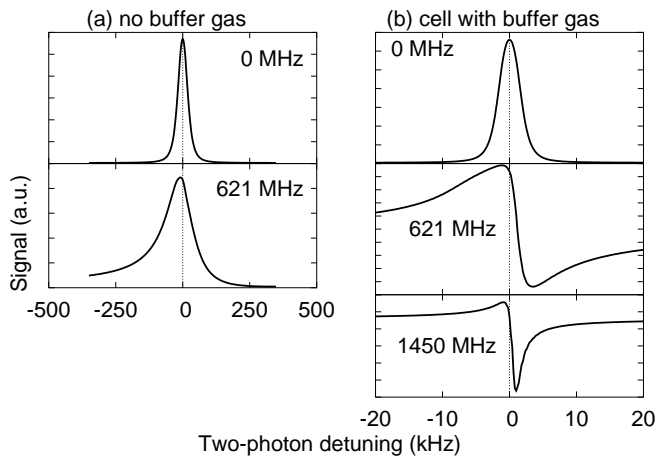


FIG. 5: Calculated transmission of probe field as a function of two-photon detuning  $\delta$  (measured in kHz) for various one-photon detunings  $\Delta$ . (a)  $^{87}\text{Rb}$  cell with no buffer gas (vacuum). (b)  $^{87}\text{Rb}$  cell with 30 Torr of Ne. The vertical scales are arbitrary.

Previous measurements involving one-photon detuning in EIT [18] differ from ours in that low laser power was used on the  $D_2$  line of Cesium, which includes a closed cycling transition, and also upper-state hyperfine structure that is covered by the Doppler width. Our numerical model shows the absence of the absorption resonance when additional homogeneous broadening parameter ( $\gamma_p$ ) is small and at low probe and drive intensity. This may be part of the reason why the absorption resonance was not observed in that work. Due to limited sensitivity of our setup we are not able to check this experimentally. The lowest total power for which we have data is  $50 \mu\text{W}$ , which is still in the power-broadened regime.

In summary, we have observed a new, isolated, narrow, two-photon absorption resonance that appears under EIT conditions when a buffer gas is used to narrow the two-photon resonance line and the one-photon detuning is comparable to or greater than the inhomogeneous Doppler linewidth. The effect occurs when homogeneous broadening (due to collisions with buffer gas) is of the order of inhomogeneous (Doppler) broadening, and the effect does not occur in the absence of buffer gas at room temperature. Although, let us note here that for cold atoms the Doppler broadening can also be of the order of or even much smaller than the homogeneous broadening, and, in this case, similar absorption resonances should be observable. This technique may provide a new tool to study BEC. Unlike previous observations of Electromagnetically Induced Absorption, this resonance does not require that the degeneracy of the ground state be lower than that of the excited state. The absorption resonance reported here is accompanied by steep anomalous dispersion giving rise to very large negative group delay.

We thank A. B. Matsko, Irina Novikova, A. M. Akul-

shin, and M. O. Scully for useful and stimulating discussions. This work was supported by the Office of Naval Research.

\* Electronic address: evmik@tamu.edu

- [1] L. V. Hau, S. E. Harris, Z. Dutton, and C. H. Behroozi, *Nature* **397**, 594 (1999).
- [2] M. M. Kash, V. A. Sautenkov, A. S. Zibrov, L. Hollberg, G. R. Welch, M. D. Lukin, Y. Rostovtsev, E. S. Fry, and M. O. Scully, *Phys. Rev. Lett.* **82**, 5229 (1999).
- [3] D. Budker, D. F. Kimball, S. M. Rochester, and V. V. Yashchuk, *Phys. Rev. Lett.* **83**, 1767 (1999).
- [4] A. Godone, F. Levi, and S. Micalizio, *Phys. Rev. A* **66**, 043804 (2002).
- [5] L. J. Wang, A. Kuzmich, and A. Dogariu, *Nature* **406**, 277 (2000).
- [6] A. M. Akulshin, A. Cimmino, A. I. Sidorov, P. Hannaford, and G. I. Opat, *Phys. Rev. A* **67**, 011801(R) (2003).
- [7] S. E. Harris and L. V. Hau, *Phys. Rev. Lett.* **82**, 4611 (1999).
- [8] D. F. Phillips, A. Fleischhauer, A. Mair, R. L. Walsworth, and M. D. Lukin, *Phys. Rev. Lett.* **86**, 783 (2001).
- [9] C. Liu, Z. Dutton, C. H. Behroozi, and L. V. Hau, *Nature* **409**, 490 (2001).
- [10] A. S. Zibrov, A. B. Matsko, O. Kocharovskaya, Y. V. Rostovtsev, G. R. Welch, and M. O. Scully, *Phys. Rev. Lett.* **88**, 103601 (2002).
- [11] S. E. Harris, *Phys. Today* **50**, 36 (1997).
- [12] A. M. Akulshin, S. Barreiro, and A. Lezama, *Phys. Rev. A* **57**, 2996 (1998).
- [13] A. V. Taichenachev, A. M. Tumaikin, and V. I. Yudin, *Phys. Rev. A* **61**, 011802 (2000).
- [14] C. Y. Ye, Y. V. Rostovtsev, A. S. Zibrov, and Y. M. Golubev, *Opt. Comm.* **207**, 227 (2002).
- [15] D. Budker, V. Yashchuk, and M. Zolotarev, *Phys. Rev. Lett.* **81**, 5788 (1998).
- [16] S. Brandt, A. Nagel, R. Wynands, and D. Meschede, *Phys. Rev. A* **56**, R1063 (1997).
- [17] M. Erhard and H. Helm, *Phys. Rev. A* **63**, 043813 (2001).
- [18] S. Knappe, M. Stähler, C. Affolderbach, A. V. Taichenachev, V. I. Yudin, and R. Wynands, *Applied Physics B* (2003).
- [19] A. V. Taichenachev, V. I. Yudin, R. Wynands, M. Stähler, J. Kitching, and L. Hollberg, accepted to *Phys. Rev. A* (2002).
- [20] Y. Dancheva, G. Alzetta, S. Cartaleva, M. Taslakov, and C. Andreeva, *Opt. Comm.* **178**, 103 (2000).
- [21] M. D. Lukin, M. Fleischhauer, A. S. Zibrov, H. G. Robinson, V. L. Velichansky, L. Hollberg, and M. O. Scully, *Phys. Rev. Lett.* **79**, 2959 (1997).
- [22] V. Sautenkov, M. Kash, V. Velichansky, and G. Welch, *Laser Physics* **9**, 889 (1999).
- [23] A. Javan, O. Kocharovskaya, H. Lee, and M. O. Scully, *Phys. Rev. A* **66**, 013805 (2002).
- [24] J. Vanier and C. Audoin, *The quantum physics of atomic frequency standards*, vol. 1 (Hilger, Bristol, 1989).
- [25] W. Happer, *Rev. Mod. Phys.* **44**, 169 (1972).